EFFECT OF COMPOSITION VARIATION WITH DEPTH ON VOLATILE OIL RESERVOIRS

By: **Ego Syahrial**

Technological Assessor at "LEMIGAS" R & D Centre for Oil and Gas Technology
Jl. Ciledug Raya Kav. 109, Cipulir, Kebayoran Lama, Jakarta Selatan 12230, Indonesia
Tromol Pos: 6022/KBYB-Jakarta 12120, Telephone: 62-21-7394422, Faxsimile: 62-21-7246150

ABSTRACT

It has been known that the distribution of hydrocarbon components in a fluid column is affected of gravity. Many authors have shown the effect of composition variation within a hydrocarbon column due to gravity. In thick reservoirs as the depth increases, the mole fraction of the lighter hydrocarbon decreases, whereas the heavy fraction increases. These variations may affect reservoir fluid properties considerably. In studying reservoir processes, especially with miscible displacements, it is essential to have of underlying mechanisms.

In this paper, we investigate the effect of composition variation with depth on volatile oil under depletion and miscible gas processes. A ternary diagram was used to identify the process displacement mechanisms at different locations. A new efficient compositional simulation approach was used to model the volatile oil reservoir bahaviour.

It was shown that the decreasing light component with depth caused different miscible displacement processes as the oil composition move toward limiting tie line in the ternary diagram. Saturation and reservoir pressures variation with depth were not linear in a thick reservoir. This non linearity increased with the increased in volatility of the oil. In the case of depletion, the concentration of light component decreased below its original composition in the produced layers. In vaporising-gas drive the light component gradually vaporized from the bottom to the top of reservoir, whereas the intermediate component decreased below its original composition from the bottom to the top of the reservoir.

Key words: *compositional, miscible, equation of state, volatile, unconditionally stable*

I. INTRODUCTION

A volatile oil[1] is defined as a high shrinkage crude oil near its critical point. In a phase diagram, it is recognised as a type between a black oil and a gas-condensate fluid. For the volatile oil, as the reservoir pressure drops below the bubble point, the reservoir flow stream becomes mostly gas and the effective permeability to oil can exhibit a rapid decline. This can often occur within a few tens or hundreds of psi below the bubble point. The thermodynamic behaviour of a volatile oil is very sensitive to pressure and temperature changes, and hence the treatment of compositional alterations is important.

It has been known that the distribution of hydrocarbon components in a fluid column is affected by gravity. Sage[2] (1938) reported that the decreasing of GOR (Gas Oil Ratio) was caused by decreasing of C_1-C_4 fraction with increasing depth and an increase of C_5 fraction with depth. Schulte[3] (1980) showed composition variations within a hydrocarbon column due to gravity. In thick reservoirs as the depth increases, the mole fraction of the lighter hydrocarbons decreases, whereas the heavy fraction increases. These variations may affect reservoir fluid properties considerably.

The calculation procedure of composition variation with depth has been proposed by Schulte[3] (1980)

and Montel[4] (1985). Schulte proposed a calculation procedure to predict composition variation with depth using Equation of State. Montel proposed a calculation procedure to predict vertical composition gradient. It was reported by Wheaton[5] (1991), the effect of ignoring compositional variation with depth was estimated to result in an error of up to 20% in estimates of hydrocarbon in-place.

In this paper, we investigate the impact of composition variation with depth on volatile oil under depletion and miscible gas processes. A ternary diagram was used to identify the process displacement mechanisms at different locations. The position of reservoir fluid in the ternary diagram will be monitored so that the expected displacement processes can be designed. A new efficient compositional simulation approach was used to model the volatile oil reservoir bahaviour. The concentration of light and intermediate component versus depth during depletion and vaporising-gas drive after simulation run will be explained.

II. MECHANISM OF MISCIBLE DISPLACEMENT

The objective of miscible displacement is to eliminate the interfacial tension between the displacing and displaced fluids so that the residual oil saturation in the swept zone can be recovered.

Some injection fluids for miscible displacement mix directly with the reservoir oil in all proportions and their mixtures remain single phase, and are said to be miscible on first contact (or first contact miscible). Other injection fluids may form two phases when mixed directly with reservoir fluids, *i.e.*, they are not first-contact miscible. However, there is in situ mass transfer between the reservoir oil and the injection fluid which forms a displacing phase with a transition zone with fluid compositions that range from pure in situ fluid to pure injection fluid composition. All intermediate compositions of this phase are continuously miscible. Miscibility achieved by in situ mass transfer of components resulting from repeated contact of oil and injection fluid during displacement is called multiple contact or dynamic miscibility[6]. Depending on the composition of the reservoir and injection fluid, dynamic miscibility is divided into two displacement processes: (i) condensing gas drive and (ii) vaporising gas drive. In condensing gas drive the mass transfer may be from gas to oil, whereas in vaporising gas drive the mass transfer is assumed to be from oil to gas. Injection fluids are typically less viscous and less dense than in situ reservoir fluids. For some reservoir configurations, injection fluid may be subject to viscous fingering and gravity segregation which can make miscible sweep efficiency disappointingly low. However, the processes can be most effectively applied in steeply dipping, high permeability reservoirs containing light oil. The objective here would be to improve miscible sweepout by taking advantage of gravity and the density difference between displacing and displaced fluids.

A. *The First-Contact Miscible Process*

Intermediate molecular weight hydrocarbons (such as propane, butane, or mixture LPG, Liquid Petroleum Gas) are frequently used for first-contact miscible flooding. In the pseudo-ternary diagram LPG is represented by the C_{2-6} pseudocomponent. First-contact miscibility can be achieved if the compositions of all mixtures of two fluids lie entirely within the single-phase region. For example as shown in Fig. 1, oil O_1 and gas G_3 or oil O_2 and gas G_2 are first contact miscible. On the other hand, oil O_1 and gas G_2 are not first contact, since some mixtures of these two fluids lie within the two-phase region.

B. *The Condensing-Gas Drive Process*

Stalkup[6] (1983) stated that for dynamic miscibility to be achieved through the condensing-gas drive method with an oil whose composition lies to the left of the critical tie line on a pseudoternary diagram, the enriched gas composition must lie to the right of the limiting tie line. For example, oil O_1 and gas G_2 will develop miscibility by multi-contact condensing drive. In this situation dynamic miscibility results from the in situ transfer of intermediate molecular weight hydrocarbons (predominantly ethane through butane) from injection gas into the reservoir oil. Natural gas at high pressures with appreciable concentrations of intermediate molecular weight hydrocarbons is used as a typical injection fluid in condensing-gas-drive and vaporizing-gas-drive flooding.

C. *The Vaporizing-Gas Drive Process*

Stalkup[6] (1983) stated that as long as the reservoir oil composition lies on, or to, the right of the critical tie line, miscibility can be attained by the vaporizing-gas drive mechanism with natural gas having a

composition lying to the left of the limiting tie-line. For example (as shown in Figure 1) oil O_2 and gas G_1 will develop miscibility by multicontact vaporising drive. In this situation dynamic miscibility relies on the in situ vaporisation of intermediate molecular weight hydrocarbons from the reservoir oil into the injected gas to create a miscible transition zone.

III. COMPOSITIONAL SIMULATION

The effect of composition variation with depth on volatile oil under depletion and miscible gas processes will be illustrated using a new compositional simulation approach[7,8]. The new formulation has an implicit equation for the oil-phase pressure and water saturation, an explicit equation for the hydrocarbon saturation, and explicit equation for the overall composition of each hydrocarbon component that satisfies thermodynamic equilibrium. The formulation uses an Equation of State for phase equilibrium and property calculations. Interfacial tension effects are included in the formulation characterise the thermodynamically dynamic nature of the relative permeability. A two-dimensional relative permeability algorithm is included which handles lumped hydrocarbon phase as well as individual phase flows.

For each grid block two equations are required, namely total hydrocarbon and water-phase flow equations. These equations are highly non-linear and they are linearised by using Newton-Raphson method. The resulting set of equations are solved by an efficient Conjugate Gradient based iterative technique to obtain pressures and saturations simultaneously, and hydrocarbon-phase saturations are deduced from their respective equations.

A. *Generalised Flow Equations*

The general flow equation used in the formulation can be found equations by summing up all the equations, applying mole constraint, and converting the resulting expressions into finite difference form namely:

- Water equation:

$$\Delta[T_w \Delta\Phi_w] + (\xi_w q_w) = \frac{V_r}{\Delta t}\left[(\phi\xi_w S_w)^{n+1} - (\phi\xi_w S_w)^n\right], \quad (1)$$

- Oil equation:

$$\Delta[T_o \Delta\Phi_o] + (\xi_o q_o) = \frac{V_r}{\Delta t}\left[(\phi\xi_o S_o)^{n+1} - (\phi\xi_o S_o)^n\right], \quad (2)$$
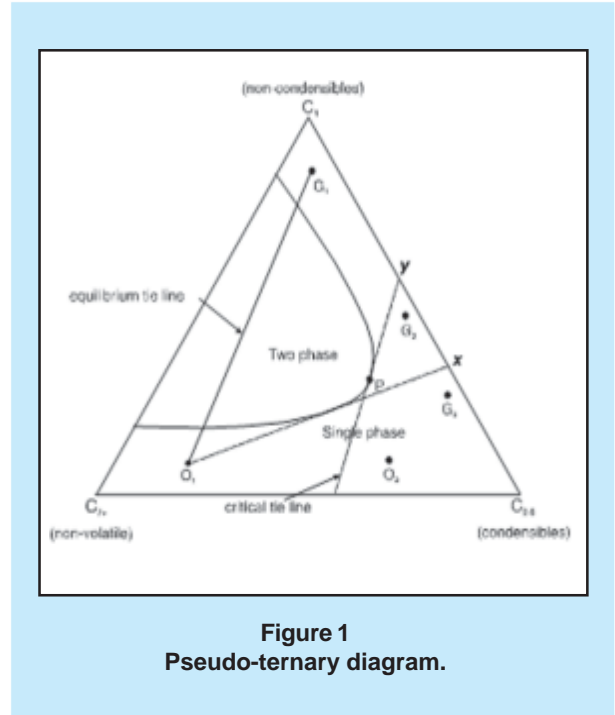
Figure 1
Pseudo-ternary diagram.

- Gas equation:

$$\Delta[T_g \Delta\Phi_g] + (\xi_g q_g) = \frac{V_r}{\Delta t}\left[(\phi\xi_g S_g)^{n+1} - (\phi\xi_g S_g)^n\right], \quad (3)$$

where transmissibility term T_l in the x-direction,

$$T_l = \left(\frac{kA}{\Delta x}\right)\left(\frac{k_{rl}}{\mu_l}\xi_l\right), \quad l = o, g, w$$

The same expression exists for y- and z-direction. In this formulation, all transmissibility term are treated implicitly. To obtain the hydrocarbon equation, both sides of oil and gas equations (Eqs. (2) and (3)) are multiplied by ξ_o^{n+1} and ξ_g^{n+1} and combined, hence:

- Hydrocarbon equation:

$$\xi_g^{n+1}\Delta[T_o^{n+1}\Delta\Phi_o^{n+1}] + \xi_o^{n+1}\Delta[T_g^{n+1}\Delta\Phi_g^{n+1}] + \xi_g^{n+1}(\xi_o q_o)^n + \xi_o^{n+1}(\xi_g q_g)^n$$
$$= \frac{V_r}{\Delta t}\left[(\phi\xi_o\xi_g S_h)^{n+1} - \xi_g^{n+1}(\phi\xi_o S_o)^n - \xi_o^{n+1}(\phi\xi_g S_g)^n\right] \quad (4)$$

where,

$$(S_h)^{n+1} = (S_o)^{n+1} + (S_g)^{n+1}$$

- Water equation:

$$\Delta[T_w^{n+1}\Delta\Phi_w^{n+1}] + (\xi_w q_w)^n = \frac{V_r}{\Delta t}\left[(\phi\xi_w S_w)^{n+1} - (\phi\xi_w S_w)^n\right] \quad (5)$$

B. Linearisation and Discretisation

It is clear that both water and hydrocarbon equations (Eqs. (4) and (5)) are highly non-linear and analytical solutions are not possible due to their complexity. Consequently, numerical methods are required. To implement numerical techniques, however, the flow equations must be linearised and the results are water and hydrocarbon equations in the oil-phase pressure and the water saturation forms.

The discretisation of water and hydrocarbon equations is carried out by applying a finite difference scheme using backward difference in time and central difference in space[9]. This results in water and hydrocarbon equations having the form:

- Water Equation:

$$
\begin{aligned}
&W_{P_{i,j,k-1}} \, \delta P_{o_{i,j,k-1}} + W_{P_{i,j-1,k}} \, \delta P_{o_{i,j-1,k}} + W_{P_{i-1,j,k}} \, \delta P_{o_{i-1,j,k}} + \\
&W_{P_{i,j,k}} \quad \delta P_{o_{i,j,k}} + W_{P_{i+1,j,k}} \, \delta P_{o_{i+1,j,k}} + W_{P_{i,j+1,k}} \, \delta P_{o_{i,j+1,k}} + \\
&W_{P_{i,j,k+1}} \, \delta P_{o_{i,j,k+1}} + W_{S_{i,j,k-1}} \, \delta S_{w_{i,j,k-1}} + W_{S_{i,j-1,k}} \, \delta S_{w_{i,j-1,k}} + \\
&W_{S_{i-1,j,k}} \, \delta S_{w_{i-1,j,k}} + W_{S_{i,j,k}} \quad \delta S_{w_{i,j,k}} + W_{S_{i+1,j,k}} \, \delta S_{w_{i+1,j,k}} + \\
&W_{S_{i,j+1,k}} \, \delta S_{w_{i,j+1,k}} + W_{S_{i,j,k+1}} \, \delta S_{w_{i,j,k+1}} = C_{rw}
\end{aligned}
\tag{6}
$$

- Hydrocarbon Equation:

$$
\tag{7}
$$

The system of equations above can be written in matrix form:

$$
A \, \delta x^{k+1} = b^k
\tag{8}
$$

where:

A = Block Hepta-diagonal Jacobian Matrix containing the coefficients on the left-hand side of Eqs. (4), and (5),

δx = The sought solutions, $[\delta P_o, \delta S_w]$

b = Vector containing the right-hand side of Eqs. (4), and (5).

This particular matrix form can be solved in each Newtonian iteration by either direct, or iterative methods in order to obtain the required changes in pressure and saturation.

C. *Composition and Saturation Equations*

Compositions are computed explicitly by a method developed by Tsutsumi and Dixon[10] (1972). The overall compositions of the components can be expressed as:

$$
z_m^{n+1} = \left[\frac{\Delta\left[x_m^{n+1}T_o^{n+1}\Delta\Phi_o^{n+1} + y_m^{n+1}T_g^{n+1}\Delta\Phi_g^{n+1}\right] + \left(x_m\xi_o q_o + y_m\xi_g q_g\right)^n + \dfrac{V_r}{\Delta t}\left[z^n\left\{(\phi\xi_o S_o) + (\phi\xi_g S_g)\right\}^n\right]}{\Delta\left[T_o^{n+1}\Delta\Phi_o^{n+1} + T_g^{n+1}\Delta\Phi_g^{n+1}\right] + \left(\xi_o q_o + \xi_g q_g\right)^n + \dfrac{V_r}{\Delta t}\left[\left\{(\phi\xi_o S_o) + (\phi\xi_g S_g)\right\}^n\right]} \right]
$$

$$
\tag{9}
$$

Oil and gas saturations are calculated as the final result of a series of computations form:

$$
S_o^{n+1} = \left[\frac{\Delta\left[T_o^{n+1}\Delta\Phi_o^{n+1}\right] + \left(\xi_o q_o\right)^n + \dfrac{V_r}{\Delta t}\left[(\phi\xi_o S_o)^n\right]}{\dfrac{V_r}{\Delta t}\left[(\phi\xi_o)^{n+1}\right]} \right] \;,
\tag{10}
$$

$$
S_g^{n+1} = \left[\frac{\Delta\left[T_g^{n+1}\Delta\Phi_g^{n+1}\right] + \left(\xi_g q_g\right)^n + \dfrac{V_r}{\Delta t}\left[(\phi\xi_g S_g)^n\right]}{\dfrac{V_r}{\Delta t}\left[(\phi\xi_g)^{n+1}\right]} \right] \;.
\tag{11}
$$

IV. DISCUSSIONS

A. *Variation of Composition and Pressure with Depth*

Fluid composition of *OIL2*[11] (composition and properties shown in Table 1) was taken from the gas oil contact at
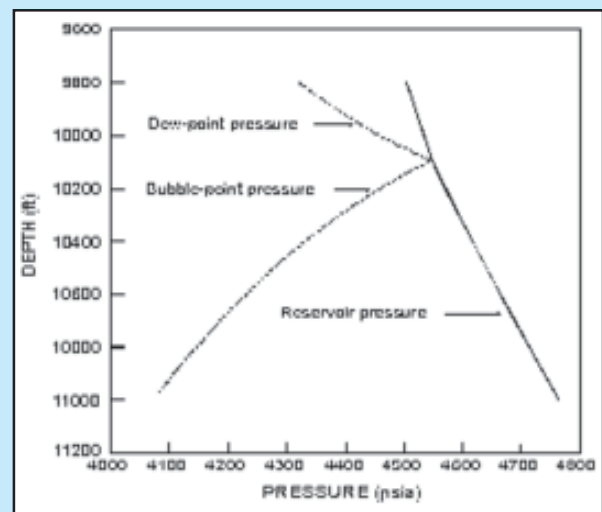
Figure 2
Pressure versus depth

Table 1
Fluid composition and properties at reservoir condition for oil2

Component	Mole Fraction	T_c (°R)	p_c (psia)	Z_c	MW	●	P_{ch}
CO_2	0.0090	548.46	1071.33	0.2741	44.01	0.225	78.0
N_2	0.0030	227.16	492.31	0.2912	28.01	0.040	41.0
C_1	0.5347	343.08	667.78	0.2847	16.04	0.013	77.0
C_2	0.1146	549.77	708.34	0.2846	30.07	0.099	108.0
C_3	0.0879	665.64	618.70	0.2775	44.10	0.152	150.3
C_4	0.0456	755.10	543.45	0.2772	58.12	0.196	187.2
C_5	0.0209	838.62	487.17	0.2688	72.15	0.241	228.9
C_6	0.0151	921.60	484.38	0.2754	84.00	0.250	271.0
Grp_1	0.0876	1034.10	436.60	0.2737	110.39	0.353	334.5
Grp_2	0.0605	1290.85	279.49	0.2474	196.70	0.633	516.6
Grp_3	0.0211	1624.60	155.26	0.2001	364.81	1.098	926.5

T_c : critical temperature; p_c : critical pressure; Z_c : critical compressibility; MW : molecular weight;

ω : acentric factor; P_{ch} : parachor.

10100 feet with 230°F and 4550 psia, and the gravity induced compositional gradient calculation option of *COMGRAD* procedure[12] has been implemented to establish vertical pressure and composition distribution with depth. Figure 2 shows the bubble-point pressure of oil zone, dew-point pressure of gas cap, and reservoir pressure versus depth for composition of *OIL2*. The maximum bubble point pressure is about 4550 psia and the minimum bubble point pressure is about 4080 psia exhibiting an approximate gradient of 0.52 psi/ft. It is also worth to note that saturation pressure and reservoir pressure variation with depth is not linear for the oil tested. This non-linearity can increase with the increase in volatility of the oil and *RFT* interpretations must be compared with this method in locating the fluid contact.

The ternary diagram was provided by *Eclipse* PVT[13] in this study. As a result of spatial variation of composition and pressure there will be different ternary diagrams at different depths. Figure 3 shows initial composition of *OIL2* at 10140 feet (just 40 feet below gas oil contact) with reservoir pressure of 4573 psia. It can be seen that this oil composition lies on the two-phase region. Therefore, both first and multiple contact miscibility cannot be achieved at this depth. Figure 4 shows initial composition of *OIL2* at 10410 feet with reservoir pressure of 4636 psia. It can be seen that condensing-gas drive can be achieved at this depth of reservoir.
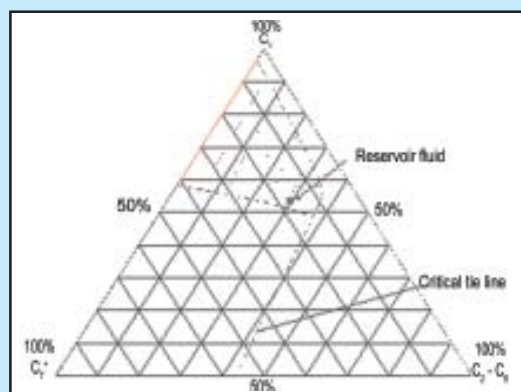
Figure 3
Ternary diagram for OIL2 at 10140 ft.
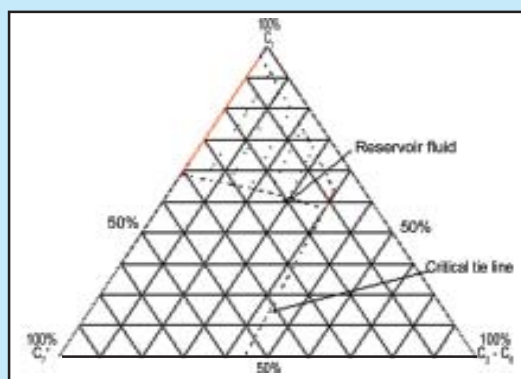
Figure 4
Ternary diagram for OIL2 at 10410 ft.

Table 2
Data used for composition variation with depth

Property	Field Units	SI Units
Grid System	20×1×20	20×1×20
Reservoir Length, L	6000 ft	1828.8 m
Reservoir Thickness, h	800 ft	243.8 m
Reservoir Width, w	100 ft	30.5 m
Reservoir Depth, D	10000 ft	3048.0 m
Permeability in x direction, k_x	100 mD	9.87×10^{-14} m^2
Permeability in z direction, k_z	100 mD	9.87×10^{-14} m^2
Porosity, ϕ	30%	30%
Initial Oil Saturation, S_{oi}	80%	80%
Initial Water Saturation, S_{wi}	20%	20%
Initial Gas Saturation, S_{gi}	0%	0%
Initial Reservoir Pressure @ Datum, p_i	5715 psia	39.4 Mpa
Datum Depth	10800 ft	3292.8 m
Depth of Gas-Oil Contact, GOC	10100 ft	3078.5 m
Oil Production Rate, q_o	5200 RB/Day	826.7 m^3/Day
Gas Production Rate, q_{gi}	5200 RB/Day	826.7 m^3/Day
Rock Compressibility, c_r	4×10^{-6} psi^{-1}	5.80×10^{-7} KPa^{-1}
Water Compressibility, c_w	3×10^{-6} psi^{-1}	4.25×10^{-7} KPa^{-1}
Viscosity of Water, μ_w	0.26 cp	0.00026 Pa.s

Tabel 3
Composition of injection gas

Composition	C_1	C_2	C_3	C_4	C_5	C_6
Mole Fraction	0.85	0.00	0.00	0.00	0.05	0.10

It is clear from these ternary diagrams that the position of reservoir oil moves towards a limiting tie line as pressure increases resulting in the suitable miscible displacement shifting from condensing to vaporizing gas drive process. In addition, pressure and temperature influence the size of the two-phase region. When pressure increases, the size of the two-phase region decreases as shown in Figure 5. This is important in terms of managing reservoirs with variable PVT properties, and identifies displacement mechanisms at different locations.
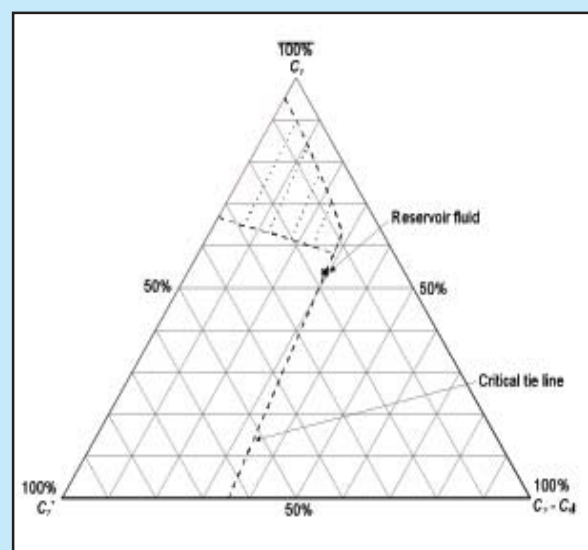
Figure 5
Ternary diagram for OIL2 at 5715 ft.
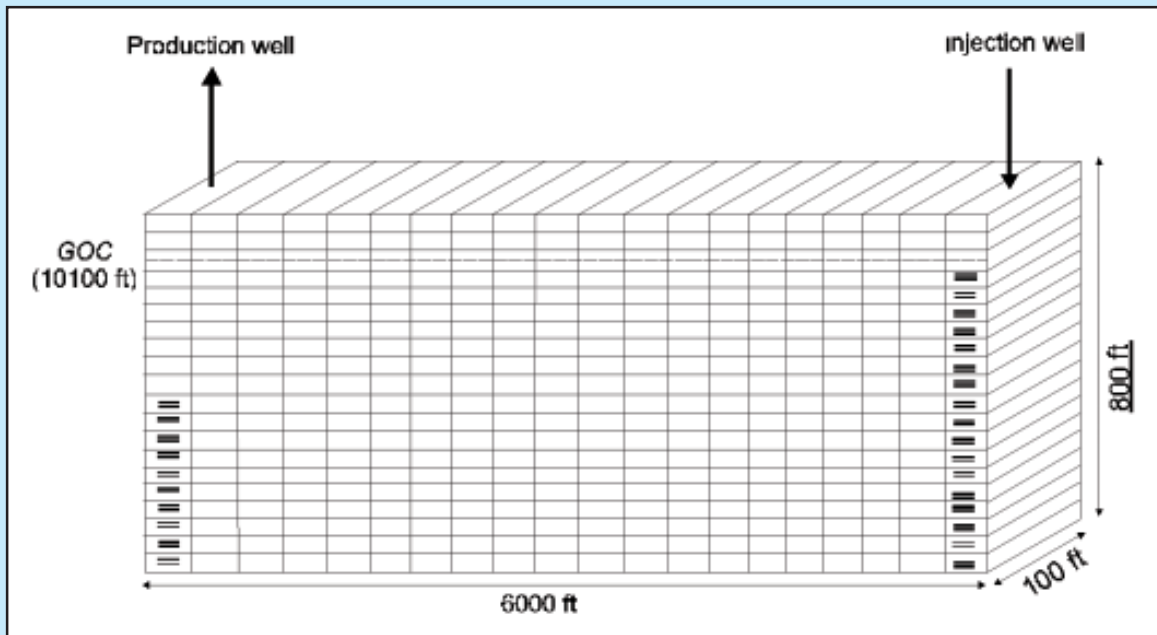
Figure 6
Schematic diagram of a two-dimensional reservoir.
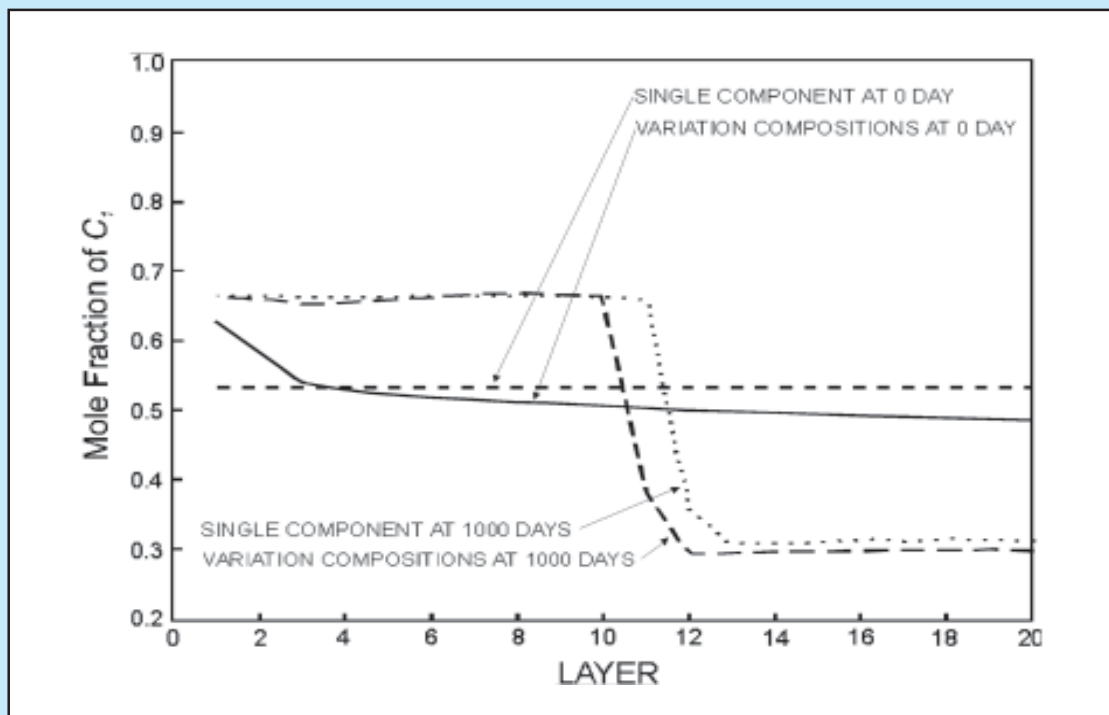
Figure 7
C_1 distribution at block 10 (x direction) in depletion processes.

Tabel 4
Variation of composition with depth

Depth (ft)	Mole Fraction of			
	$N_2 - C_1$	$CO_2 - C_2$	$C_3 - C_6$	$Grp_1 - Grp_3$
10000.0	0.6561	0.1285	0.1462	0.0691
10071.4	0.6473	0.1287	0.1491	0.0750
10100.0	0.5377	0.1236	0.1695	0.1692
10250.0	0.5189	0.1216	0.1704	0.1891
10392.9	0.5078	0.1203	0.1705	0.2013
10500.0	0.5012	0.1195	0.1705	0.2089
10642.9	0.4936	0.1185	0.1704	0.2175
10750.0	0.4886	0.1178	0.1702	0.2234
10892.9	0.4826	0.1170	0.1700	0.2234

$C_3 - C_6$ contains of C_3, C_4, C_5 and C_6 ; $Grp_1 - Grp_3$ contains of Grp_1, Grp_2 and Grp_3
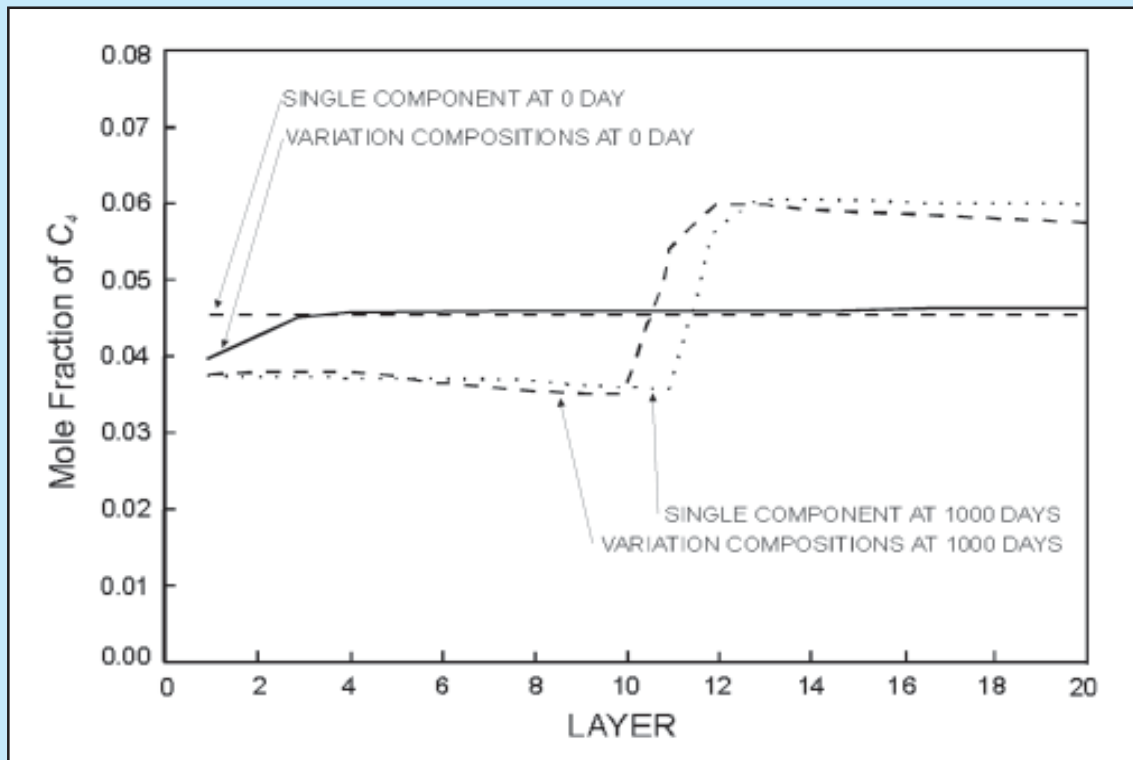
Figure 8
C_4 distribution at block 10 (x direction) in depletion processes
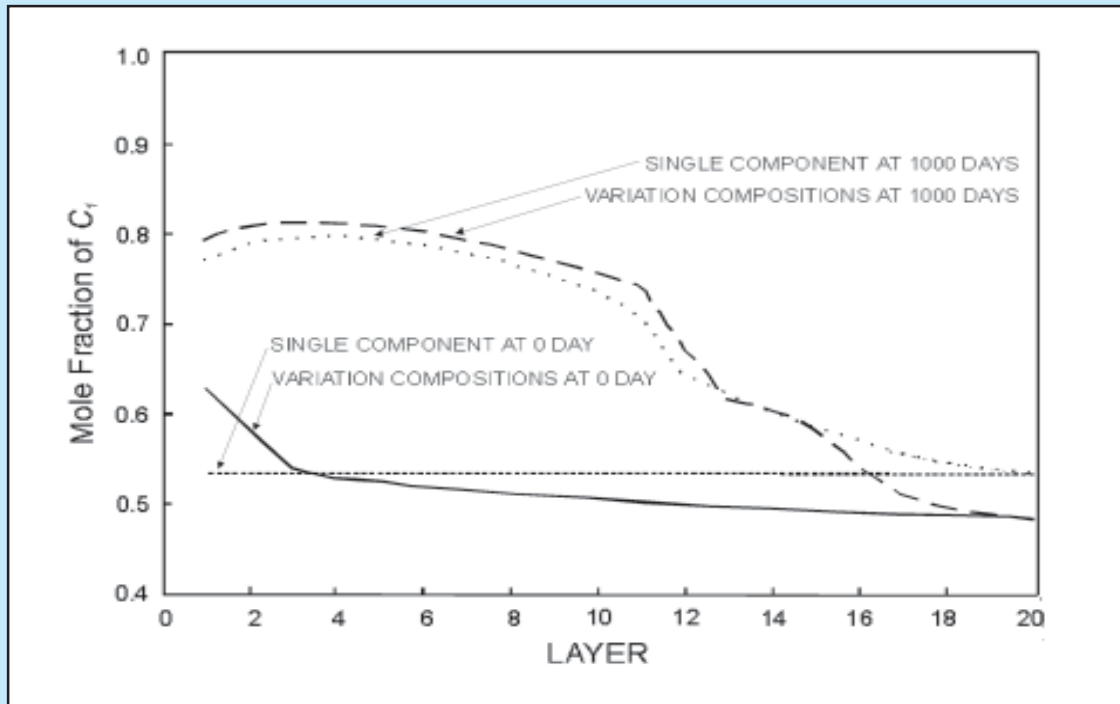
Figure 9
C_1 distribution at block 10 (x direction) in vaporising-gas drive
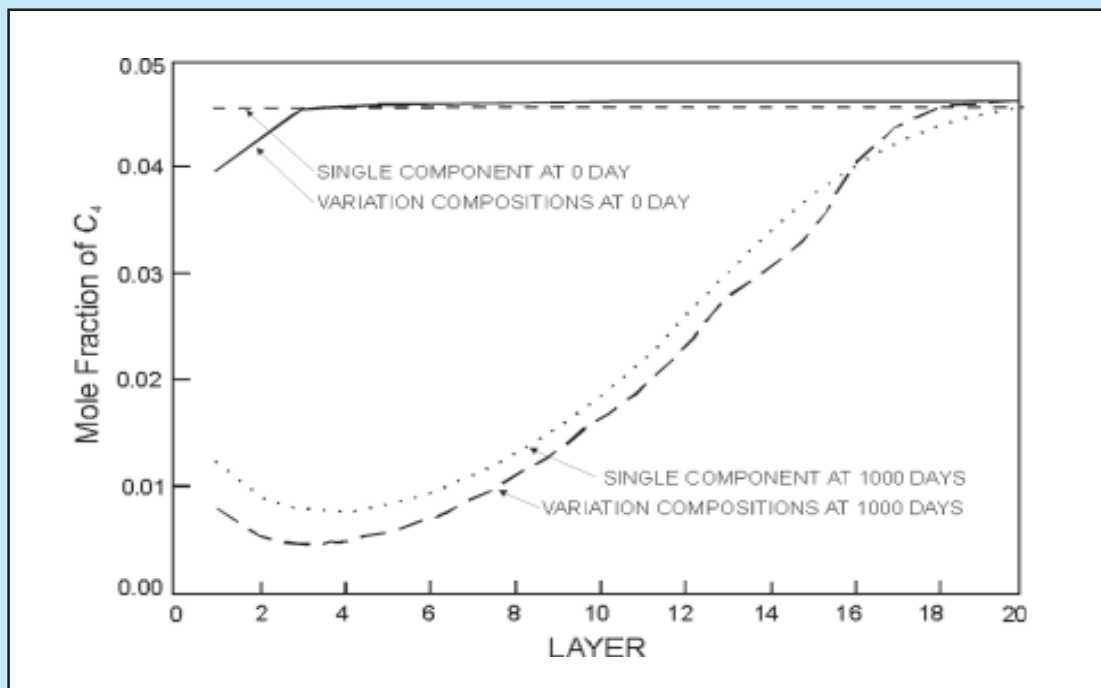
Figure 10
C_4 distribution at block 10 (x direction) in vaporising-gas drive.\
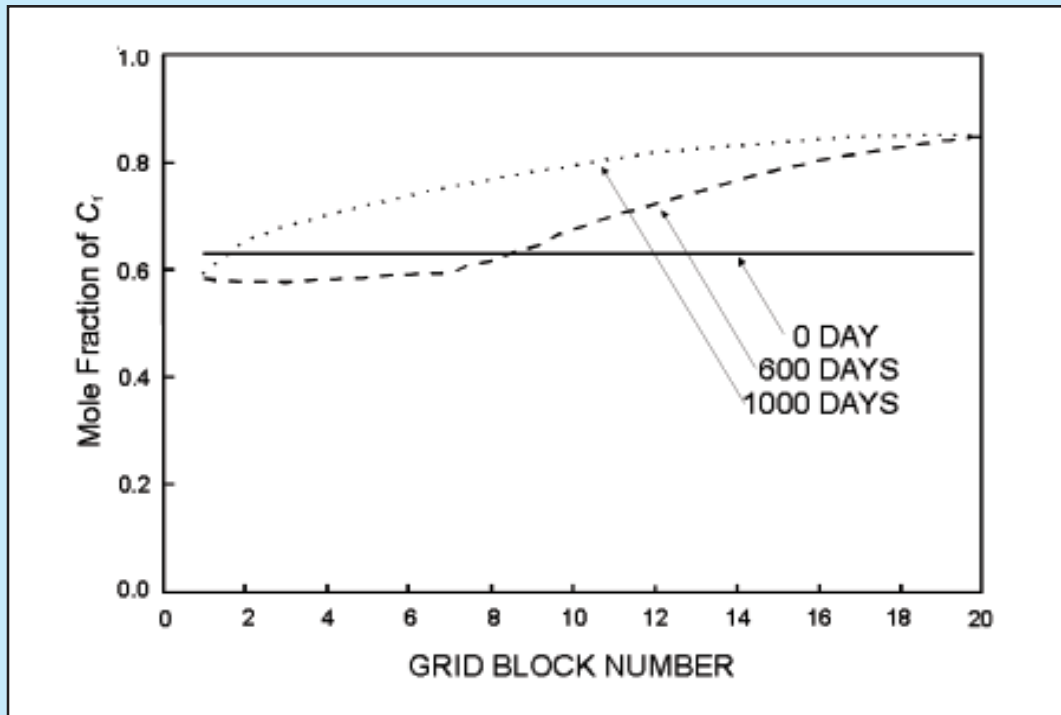
Figure 11
C$_1$ distribution in the top of reservoir
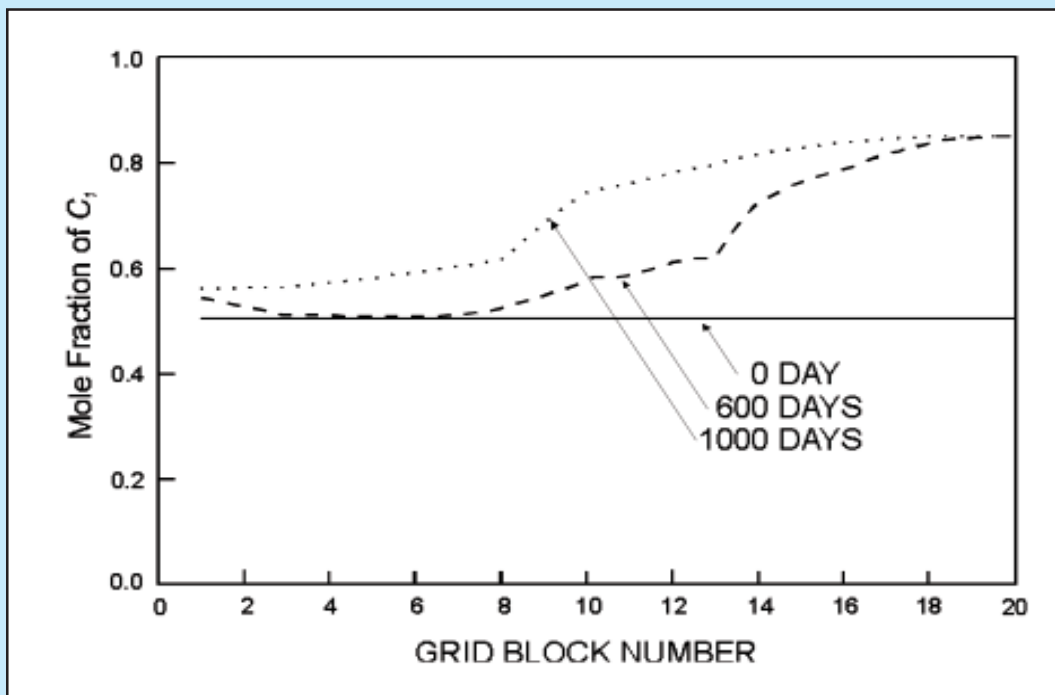
Figure 12
C$_1$ distribution in the middle of reservoir

B. *Cross-Sectional Studies in Homogeneous and Horizontal Reservoirs*

In this section, a two-dimensional cross sectional reservoir model was build to investigate the influence of composition with depth on the depletion and miscible displacement performance of the volatile oil reservoirs. The reservoir domain selected for the purposes is shown in Figure 6. The reservoir is 6000 ft long, 100 ft wide and has a thickness of 800 ft. The model is represented by a 20´1´20 grid and the other input data are listed in Table 1 and Table 2. Using fluid composition of *OIL2* obtained from the gas oil contact at 10100 ft, the compositional gradient calculation option from *COMGRAD*

Figure 13
C$_1$ distribution in the bottom of reservoir

procedure is implemented to obtain spatial variation of composition with depth and some of the results are listed Table 4.

The first model is a depletion process where the production well penetrates layer 11 to layer 20 in block 1. With the reservoir production rate of 5200 RB/Day and initial reservoir pressure of 5715 psia, the model is run for 1000 days. The second model is a vaporizing-gas drive where the injection well penetrates layer 4 to layer 20 in block 20 and the production well penetrates layer 11 to 20 in block 1 as shown in Figure 6. Production and injection rates are set 5200 RB/Day. To assess the change in total mole fraction of light components with production over a reasonable time period, the model is run with constant composition with depth.

Figs. 7 through 10 show the distribution of light C_1 and intermediate C_4 from the top to the bottom reservoir in block 10 (*x*-direction) after 1000 days of flow in depletion and vaporizing-gas drive. In case of depletion, the concentration of light component decreases below its original composition and the intermediate component increases above its original composition in the layers produced as shown in Figs. 7 and 8. In vaporizing-gas drive as shown in Figs. 9 and 10, the light component gradually vaporizes from

the bottom to the top of reservoir, whereas the intermediate component decreases below its original composition from the bottom to the top of reservoir.

The most important aspect in the thick reservoir with variation in composition is the displacement mechanisms at different depth. It is clear that decreasing of light component with depth will cause different miscible displacement efficiency, since the oil compositions move towards limiting tie line in ternary diagram. Figs. 11 through 13 show how the total mole fraction of each component change from injection well to producing well in top, middle, and bottom reservoir. These will cause different gas breakthrough times with depth in the producing well.

V. CONCLUSIONS

1. Saturation and reservoir pressure with depth are not linear and this non-linearity increased with the increase in volatlity of the oil.

2. In the presence of spatial property variation in volatile oil reservoirs, the interaction of the injected gas with in situ oil can be different at different spatial locations. At one depth one could achieve condensing and at another depth one could achieve vaporising gas drive with the same injected gas.

3. In case of depletion, the concentration of light component decreased below its original composition and the intermediate component increased above its original composition in the produced layers.

4. In the vaporising-gas drive the light component gradually vaporized from the bottom to the top of the reservoir, whereas the intermediate component decreased below its original composition from the bottom to the top of the reservoir.

5. The decreasing light component with depth caused different miscible displacement processes as the oil composition moved towards the limiting tie line in the ternary diagram.

REFERENCES

1. Moses, P.L.: "Engineering Applications of Phase Behaviour of Crude Oil and Condensate Systems," J.P. Tech., (July 1986), 38, 715-723.

2. Sage, B.H. and Lacey, W.N.: "Gravitational Concentration Gradients in Static Columns of Hydrocarbon Fluids," Trans. AIME (1939), 132, 120-131.

3. Schulte, A.M.: "Compositional Variations within a Hydrocarbon Column due to Gravity," paper SPE 9235, Proc. 55th Annual Fall Technical Conference and Exhibition of the SPE of AIME, Dallas, Texas, (Sept. 21-24, 1980).

4. Montel, F. and Gouel, P.L.: "Prediction of Compositional Grading in a Reservoir Fluid Column", SPE 14410, presented at the 1985 Annual Technical Conference and Exhibition, Las Vegas, September 22-25.

5. Wheaton, R.J.: "Treatment of Variations of Composition with Depth in Gas-Condensate Reservoir," SPE, Reservoir Engineering, May 1991, 239-244.

6. Stalkup, F.I.: Miscible Flooding, Monograph 8, SPE, Richardson, Texas, USA (1983).

7. Syahrial, E. and Daltaban, T.S.: "A New Compositional Simulation Approach to Model Recovery from Volatile Oil Reservoirs", paper SPE 39757, the 1998 SPE Asia Pacific Conference on Integrated Modelling for Asset Management held in Kuala Lumpur, Malaysia, 23-24 March 1998.

8. Syahrial, E. and Daltaban, T.S.: "Development of A Novel Compositional Simulation Approach to Model Recovery from Volatile Oil Reservoirs", presented in the 26th Annual Convention & Gas Habitats of SE Asia and Australia Conference held in Jakarta, Indonesia, 27-29 October 1998.

9. Peaceman, D.W.: Fundamentals of Numerical Simulation, Elsevier Scientific Publishing Co., Amsterdam Nedertland (1967).

10. Tsutsumi, G. and Dixon, T.N.: "Numerical Simulation of Two-Phase Flow With Interphase Mass Transfer In Petroleum Reservoirs," paper SPE, Proc. SPE-AIME 47th Annual Fall Meeting, San Antonio (Oct. 8-11, 1972).

11. Coats, K.H. and Smart, G.T.: "Application Of A Regression Based EOS PVT Programe To Laboratory Data," paper SPE 11197, Proc. 57th Annual Fall Technical Conference and Exhibition of the SPE of AIME, New Orleans, Los Angeles, (Sept. 26-29, 1982).

12. Daltaban, T.S.: "Private Comumunication," (1996).

13. GeoQuest, Schlumberger: "Eclipse PVT: Reference Manual," Version 96A, (1996).˅